Electronic Structure of the Lowest Excited States of $Cr(CO)_4$(2,2′-bipyridine): A CASSCF/CASPT2 Analysis

Dominique Guillaumont,[†] Chantal Daniel,*[,†] and Antonín Vlček, Jr.[‡,§]

Laboratoire de Chimie Quantique, UPR 139 du CNRS, Institut Le Bel, Université Louis Pasteur, 4 rue Blaise Pascal, 67000 Strasbourg, France, and J. Heyrovský Institute of Physical Chemistry, Academy of Sciences of the Czech Republic, Dolejškova 3, 182 23 Prague, Czech Republic

Received July 22, 1996[⊗]

The visible and UV absorption spectra of $Cr(CO)_4$(bpy) are interpreted according to CASPT2 calculations based on CASSCF reference wave functions using atomic natural orbital (ANO) basis sets. The excitation energies of the lowest singlet MLCT (metal-to-ligand-charge-transfer) states range between 12 630 and 17 580 cm^{-1}. They originate in the excitation of chromium d electrons to the lowest π^*_{bpy} orbital of b_2 local symmetry. Dipole transition moments calculated for individual MLCT transitions show that the only transition expected to contribute significantly to the intense absorption band in the visible spectral region is the $a^1A_1 \rightarrow b^1A_1$ transition calculated at 17 580 cm^{-1}. This result agrees very well with the experimental spectra recorded in weakly solvating C_2Cl_4, characterized by a band at 17 700 cm^{-1}. The low-energy emission band at 12 850 cm^{-1} has been attributed to the lowest a^3B_2 state calculated at 12 560 cm^{-1}. The next set of excited states corresponding to $3d \rightarrow \pi^*_{bpy,a_2}$ excitations range between 25 370 and 26 200 cm^{-1} for the singlets and between 24 630 and 25 750 cm^{-1} for the triplets. The singlet excited states corresponding to $d \rightarrow d$ excitations are calculated between 29 650 and 37 360 cm^{-1}. These results show that the intense absorption in the near-UV spectral region originates in strongly overlapping absorption bands due to closely spaced transitions into MLCT (a_2) and dd excited states, respectively. The c^1B_2 excited state corresponding to the $3d_{xz} \rightarrow 3d_{z^2}$ excitation, proposed as photoactive in the mechanism of the efficient CO loss under irradiation at 27 630 cm^{-1}, is calculated at 36 320 cm^{-1} and is far too high to be directly populated in these photochemical studies. Its mixing with one or several low-lying (singlet) MLCT states at the early stage of the reaction path could be responsible for the observed primary reaction. A comparison between the excitation energies of the lowest singlet states of $Cr(CO)_4$(bpy) and $Cr(CO)_4$(dab) is reported. The most significant feature is the lowering of the MLCT excited states on going from the bpy-containing molecule to its dab (1,4-diaza-1,3-butadiene) analog.

Introduction

Transition metal carbonyls with low-lying MLCT states exhibit specific photochemical and photophysical properties which may be used to promote different applications such as energy/electron transfer processes or photosubstitution reactions.[1−3] The detailed mechanism of the CO photosubstitution in this class of molecules, of which $Cr(CO)_4$(bpy) is representative, sustains a longstanding controversy.[4−15] Despite of the experimental activity performed in this field in the past 10 years, many unknowns still remain regarding the nature of the reactive excited states (metal centered, MLCT), the role of the low-lying triplet excited states, the mixing of different types of excited states along the metal−CO elongation, and the excited state dynamics.

The quantum yield Φ of the photosubstitution reaction

$$Cr(CO)_4(bpy) + PPh_3 \xrightarrow{h\nu} Cr(CO)_3(PPh_3)(bpy) + CO \quad (1)$$

has been measured with high precision as a function of the irradiation wavelength in different solvents.[12,13] Pressure dependence of quantum yields at different wavelengths of excitation was studied for an analogous photosubstitution of $Cr(CO)_4$(phen) by phosphines and phosphites.[5,15] According to these experiments, the photosubstitution quantum yields decrease abruptly with decreasing excitation energies in the near-UV region, followed by a slow, nearly linear decrease in the visible region corresponding to the MLCT absorption. The reaction (1) is rather efficient ($\Phi \geq 10^{-2}$) on irradiation into the visible MLCT absorption band (532 nm or 18 800 cm^{-1}). These results have been rationalized as follows: (i) the photosubstitution reaction (1) follows a dissociative mechanism regardless of the excitation wavelengths; (ii) direct irradiation into the dissociative excited states corresponding to $d \rightarrow d$ excitations leads to a

† Université Louis Pasteur.
‡ Academy of Sciences of the Czech Republic.
§ Present address: Department of Chemistry, Queen Mary and Westfield College, University of London, London E1 4NS, U.K.
⊗ Abstract published in *Advance ACS Abstracts,* March 15, 1997.

(1) Meyer, T. J. *Pure Appl. Chem.* **1986**, *58*, 1193.
(2) Lees, A. J. *Chem. Rev* **1987**, *87*, 711.
(3) Stufkens, D. J. *Coord. Chem. Rev.* **1990**, *104*, 39.
(4) Wrighton, M. S.; Morse, D. L. *J. Organomet. Chem.* **1975**, *97*, 405.
(5) Wieland, S.; Bal Reddy, K.; van Eldik, R. *Organometallics* **1990**, *9*, 1802.
(6) Manuta, D. M.; Lees, A. J. *Inorg. Chem.* **1986**, *25*, 1354.
(7) Balk, R. W.; Snoeck, T.; Stufkens, D. J.; Oskam, A. *Inorg. Chem.* **1980**, *19*, 3015.
(8) Johnson, C. E.; Trogler, W. C. *J. Am. Chem. Soc.* **1981**, *103*, 6352.
(9) Trogler, W. C. In *Excited States and Reactive Intermediates*; Lever, A. B. P., Ed.; ACS Symposium Series 307; American Chemistry Society: Washington, DC, 1986; p 177.
(10) Lees, A. J.; Fobare, J. M.; Mattimore, E. F. *Inorg. Chem.* **1984**, *23*, 2709.
(11) van Dijk, H. K.; Stufkens, D. J.; Oskam, A. *J. Am. Chem. Soc.* **1989**, *111*, 541.
(12) Víchová, J.; Hartl, F.; Vlček, A., Jr. *J. Am. Chem. Soc.* **1992**, *114*, 10903.
(13) Vlček, A., Jr.; Víchová, J.; Hartl, F. *Coord. Chem. Rev.* **1994**, *132*, 167.
(14) Virrels, I. G.; George, M. W.; Turner, J. J.; Peters, J.; Vlček, A., Jr. *Organometallics* **1996**, *15*, 4089.
(15) Wen-Fu, F.; van Eldik, R. *Inorg. Chim. Acta*, in press.

S0020-1669(96)00872-5 CCC: $14.00

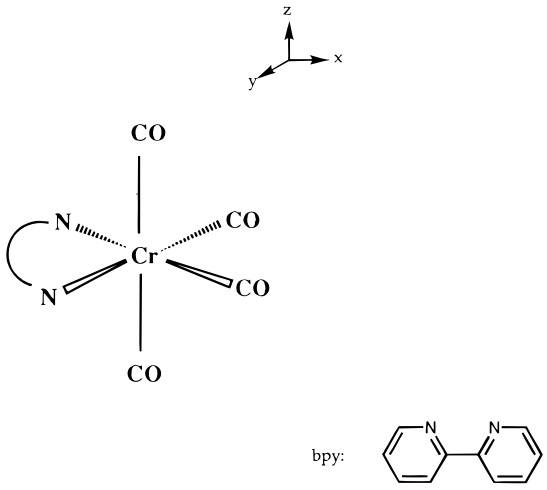

Figure 1. Idealized molecular structure of $Cr(CO)_4(bpy)$.

very efficient CO loss; (iii) a lower quantum yield CO loss occurs from directly excited (near) Franck−Condon vibronic levels of the ^{1}MLCT state, competitively with the vibrational relaxation. A simple analysis in terms of bonding and antibonding molecular orbitals involved in these excited states has proposed a b_2 asymmetric vibronic activation of the M−CO bond by the optical excitation.[13] A mixing of the metal-centered and MLCT states may result from this asymmetric distortion. This rather qualitative explanation has to be enhanced by more sophisticated theoretical studies, which could lead to more general model of a ligand dissociation on MLCT excitation. A DV−Xα study[16] of the lowest excited states of the title molecule predicted the lowest MLCT excited states at about 23 000−30 103 cm^{-1} and the lowest bpy (π π^*) excitations at 36 000 and 42 000−45 000 cm^{-1}. The calculated excitation energies were not improved by a subsequent CI treatment and remained overestimated by more than 0.5 eV with respect to the reported experimental visible absorption band between 17 700 and 19 750 cm^{-1}.

The aim of the present study is to investigate the nature and the relative order of the low-lying excited states of $Cr(CO)_4$-(bpy) on the basis of CASSCF/LS-CASPT2 calculations and to assign the experimental absorption spectrum. Recent theoretical studies reported for the calculation of excited states in transition metal compounds have shown that the CASSCF/CASPT2 approach gives results in rather good agreement with the experimental spectra when available.[17−20] Another goal of this work is to define a starting point for a subsequent study of the photodissociation of $Cr(CO)_4(bpy)$ on the basis of state correlation diagrams and potential energy curves.

Computational Method

The C_{2v} geometry (with O_x the C_2 axis) of $Cr(CO)_4(bpy)$ has been idealized from the experimental structures of Ru(bipyridine)$_3^{2+}$ [21] and $Cr(CO)_6$[22] (Figure 1), the bond distances and angles being those used in the previous DV−Xα study.[16] The

Chart 1

bpy dab

basis sets which are of generally contracted atomic natural orbital (ANO) type[23] are the following:[24] for the chromium atom a (17,12,9) set contracted to [6,4,3], for the first-row atoms a (10,6) set contracted to [3,2], and for hydrogen atoms a (7) set contracted to [2].

Complete active space SCF (CASSCF)[25] calculations were carried out to obtain wave functions which are used as references in the second-order perturbation calculation.[26] The natural orbitals of CASSCF wave functions, averaged over the lowest (two or three) states of a given symmetry, form the one-electron basis of the CASPT2 which provides the first-order wave function and the second-order energy in the full space of configurations generated by this basis. In the CASPT2 calculation, only the valence electrons, namely the metal 3d and the second-row atoms 2s and 2p electrons, were correlated. Since our interest centers mostly on the lowest excited states of $Cr(CO)_4(bpy)$ corresponding to 3d $\rightarrow$ π^*_{bpy} and 3d $\rightarrow$ 3d excitations, mainly the 3d orbitals and the 4d which correlate them, the lowest bpy π^* (b_2 and a_2) orbitals, and doubly occupied orbitals with a significant metal contribution were included in the CASSCF active space. Ten electrons are correlated in 11 (or 12 when the bpy $\pi^*(a_2)$ orbital is included) active orbitals. A level shift corrected version of the original CASPT2 program (so-called LS-CASPT2) was used in order to avoid intruder states problems.[27]

In order to determine a coherent strategy for a subsequent study of the CO photodissociation pathway (reaction 1), several calculations were performed for the less crowded model system $Cr(CO)_4L$ (with L = dab = 1,4-diaza-1,3-butadiene) (Chart 1) on the basis of 8e10a CASSCF wave functions, the dynamic part of the correlation energy having been taken into account either at the CASPT2 level using ANO basis sets, as described above, or at the CCI level[28] using Wachters type basis sets as follow: for the chromium atom a (15,11,6) set contracted to [9,6,3],[30] for the first-row atoms a (10,6) set contracted to [4,2],[32] and for hydrogen a (4) set contracted to [2].[33]

The calculations were performed either with the MOLCAS-3 quantum chemistry software[34] on an IBM RS6000/390 worksta-

(16) Kobayashi, H.; Kaizu, Y.; Kimura, H.; Matzuzawa, H.; Adachi, H. *Mol. Phys*. **1988**, *6*, 1009.
(17) Pierloot, K.; van Praat, E.; Vanquickenborne, L. G.; Roos, B. J. *J. Phys. Chem.* **1993**, *97*, 12220.
(18) Persson, B. J.; Roos, B. O.; Pierloot, K. *J. Chem. Phys.* **1994**, *101*, 6810.
(19) Roos, B. O.; Andersson, K.; Fülscher, M. P.; Malmqvist, P. A.; Serrano-Andres, L.; Pierloot, K.; Merchan, M. *Adv. Chem. Phys.* **1996**, *93*, 219.
(20) Heitz, M. C.; Daniel, C. *Chem. Phys. Lett.* **1995**, *246*, 488.
(21) Rillence, D. P.; Jones, D. S.; Levy, H. A. *J. Chem. Soc., Chem. Commun.* **1979**, 849.
(22) Jost, A.; Rees, B.; Yelon, W. B. *Acta Crystallogr*. **1975**, *B31*, 2649.
(23) Almlöf, J.; Taylor, P. R. *J. Chem. Phys.* **1987**, *86*, 4070.
(24) Pierloot, K.; Dummez, B.; Widmark, P. O.; Roos, B. O. *Theor. Chim. Acta* **1995**, *90*, 87.
(25) Siegbahn, P. E. M.; Almlöf, J.; Heiberg, A.; Roos, B. O. *J. Chem. Phys.* **1981**, *74*, 2384.
(26) Andersson, K.; Roos, B. O. *Int. J. Quantum Chem.* **1993**, *45*, 591 and references therein.
(27) Roos, B. O.; Andersson, K. *Chem. Phys. Lett.* **1995**, *245*, 215.
(28) Siegbahn, P. E. M. *Int. J. Quantum Chem.* **1983**, *23*, 1869. The original program was interfaced for use in conjunction with the ASTERIX system of programs[29] by C. Daniel, M. Speri, and M. M. Rohmer.
(29) Ernenwein, R.; Rohmer, M. M.; Bénard, M. *Comput. Phys. Commun.* **1990**, *58*, 305. Rohmer, M. M.; Demuynck, J.; Bénard, M.; Wiest, R.; Bachmann, C.; Henriet, C.; Ernenwein, R. *Comput. Phys. Commun.* **1990**, *60*, 127. Wiest, R.; Demuynck, J.; Bénard, M.; Rohmer, M. M.; Ernenwein, R. *Comput. Phys. Commun.* **1991**, *62*, 107.
(30) This basis set is made from the (14,9,5) basis set of Wachters (Wachters, A. J. H. *J. Chem. Phys.* **1970**, *52*, 1033) by adding an additional s function (exponent 0.3218), two diffuse p functions, and one diffuse d function. All the exponents were chosen according to the even-tempered criterion of Raffenetti.[31]
(31) Raffenetti, R. C., McRae, W. B., Eds.; Wiley: New York, 1973; p 164.
(32) Huzinaga, S. *Approximate Atomic Functions*; Technical Report; University of Alberta: Alberta, Canada, 1971.
(33) Huzinaga, S. *J. Chem. Phys*. **1965**, *42*, 1293.

Table 1. CASSCF and CASPT2 Total Energies (in hartrees) of the $Cr(CO)_4(bpy)$ Electronic Ground State, Lowest MLCT and Metal-Centered Excited States, and Corresponding Weights ω of the First-Order Reference Wave Function in CASPT2

state	principal configuration	CASSCF[a]	CASPT2	ω
d^1A_1	$(3d_{xz})^2(3d_{yz})^2(3d_{x^2-y^2})1(3d_{z^2})^1$	−1986.07639 (0.69)	−1987.91734	0.710
c^1B_2	$(3d_{xz})^1(3d_{yz})^2(3d_{x^2-y^2})^2(3d_{z^2})^1$	−1986.07596 (0.61)	−1987.92207	0.709
b^1B_2	$(3d_{xz})^2(3d_{yz})^1(3d_{x^2-y^2})^2(3d_{xy})^1$	−1986.09596 (0.65)	−1987.93615	0.710
c^3B_2	$(3d_{xz})^1(3d_{yz})^2(3d_{x^2-y^2})^2(3d_{z^2})^1$	−1986.10395 (0.67)	−1987.94390	0.710
c^3A_1	$(3d_{xz})^2(3d_{yz})^2(3d_{x^2-y^2})^1(3d_{z^2})^1$	−1986.10777 (0.88)	−1987.94695	0.711
c^1B_1	$(3d_{xz})^2(3d_{yz})^2(3d_{x^2-y^2})^1(3d_{xy})^1$	−1986.11577 (0.91)	−1987.95245	0.711
b^3B^2	$(3d_{xz})^2(3d_{yz})^1(3d_{x^2-y^2})^2(3d_{xy})^1$	−1986.12366 (0.83)	−1987.95895	0.711
b^1B_1	$(3d_{xz})^1(3d_{yz})^2(3d_{x^2-y^2})^2(\pi^*_{bpy,a_2})^1$	−1986.13319 (0.84)[b]	−1987.96982[b]	0.711
b^3B_1	$(3d_{xz})^1(3d_{yz})^2(3d_{x^2-y^2})^2(\pi^*_{bpy,a_2})^1$	−1986.13549 (0.84)[b]	−1987.97188[b]	0.711
c^1A_1	$(3d_{xz})^2(3d_{yz})^1(3d_{x^2-y^2})^2(\pi^*_{bpy,a_2})^1$	−1986.13512 (0.82)[b]	−1987.97363[b]	0.713
b^3A_1	$(3d_{xz})^2(3d_{yz})^1(3d_{x^2-y^2})^2(\pi^*_{bpy,a_2})^1$	−1986.14117 (0.84)[b]	−1987.97701[b]	0.711
b^3B_1	$(3d_{xz})^2(3d_{yz})^2(3d_{x^2-y^2})^1(3d_{xy})^1$	−1986.14216 (0.91)	−1987.97786	0.711
b^1A_1	$(3d_{xz})^1(3d_{yz})^2(3d_{x^2-y^2})^2(\pi^*_{bpy,b_2})^1$	−1986.16868 (0.87)	−1988.00746	0.710
a^3A_1	$(3d_{xz})^1(3d_{yz})^2(3d_{x^2-y^2})^2(\pi^*_{bpy,b_2})^1$	−1986.17317 (0.88)	−1988.01554	0.711
a^1B_1	$(3d_{xz})^2(3d_{yz})^1(3d_{x^2-y^2})^2(\pi^*_{bpy,b_2})^1$	−1986.18870 (0.90)	−1988.02172	0.712
a^3B_1	$(3d_{xz})^2(3d_{yz})^1(3d_{x^2-y^2})^2(\pi^*_{bpy,b_2})^1$	−1986.18970 (0.87)	−1988.02546	0.711
a^1B_2	$(3d_{xz})^2(3d_{yz})^2(3d_{x^2-y^2})^1(\pi^*_{bpy,b_2})^1$	−1986.18496 (0.87)	−1988.03002	0.709
a^3B_2	$(3d_{xz})^2(3d_{yz})^2(3d_{x^2-y^2})^1(\pi^*_{bpy,b_2})^1$	−1986.18408 (0.85)	−1988.03035	0.709
a^1A_1	$(3d_{xz})^2(3d_{yz})^2(3d_{x^2-y^2})^2$	−1986.27156 (0.91)	−1988.08756	0.715
		−1986.26598[b]	−1988.08922[b]	0.713

[a] In parentheses are reported the CASSCF coefficients on the principal configuration. [b] CASSCF including the π^*_{bpy,a_2} orbital in the active space.

tion or with the coupled systems of programs ARGOS[35] and ASTERIX[29] interfaced to the CCI.[28]

Experimental Details

The $Cr(CO)_4(bpy)$ complex was prepared by a previously published procedure[36] and recrystallized from a CH_2Cl_2−isooctane mixture under a nitrogen atmosphere. The solvents used were purified as described in ref 13. Absorption spectra were recorded for degassed solutions under an argon atmosphere on a Carl-Zeiss-Jena M40 spectrophotometer. The diffuse reflectance spectrum was recorded for $Cr(CO)_4(bpy)$ dispersed in a KNO_3 pellet on a Perkin-Elmer Lambda 19 spectrophotometer equipped with a 60 mm integrating sphere, model B013-9941.

Results and Discussion

$CrCO)_4(bpy)$ Absorption/Emission Spectra. $Cr(CO)_4(bpy)$ exhibits[6,7,12,13,37,38] an intense absorption band in the visible region and even stronger absorption in the UV region, at energies above ca. 22 000 cm^{-1}. The position and extinction coefficient of the visible absorption band is strongly solvent dependent: $C_2H_2Cl_2$, 19 750 cm^{-1}, 3715 M^{-1} cm^{-1}; C_6H_6, 18 900 cm^{-1}, 3970 M^{-1} cm^{-1}; toluene, 18 690 cm^{-1}, 4196 M^{-1} cm^{-1}; 6/1 (v/v) C_2Cl_4/C_6H_6 mixture, 17 700 cm^{-1}, 4411 M^{-1} cm^{-1}. The bandwidth is rather large, ca. 3400 cm^{-1} in toluene. On the basis of this strong solvatochromism[6,7,38] and the ligand substituents' dependence,[6] the visible absorption band was attributed to the MLCT transition(s). This conclusion is supported by a close correspondence between the resonance Raman spectra[39] of $Cr(CO)_4(bpy)$ and $Ru(bpy)_3^{2+}$. Qualitative molecular orbital arguments show[3,40] that the $d_{xz} \rightarrow \pi^*_{bpy,b_2}$ transition should be the most important contributor to the MLCT absorption because of the overlap between these two orbitals. The only indication for a presence of low-lying MLCT transitions of a different orbital origin comes from the diffuse reflectance spectrum of solid $Cr(CO)_4(bpy)$ which shows a weak "tail" between ca. 680 and 780 nm (14 710 and 12 820 cm^{-1}). MLCT absorptions for $Cr(CO)_4(R\text{-}dab)$ complexes[7,40] (R-dab = R−N═CH−CH═N−R) occur at lower energies than those for $Cr(CO)_4(bpy)$. For example, a strong band at 17 700 cm^{-1} was found in C_6H_6 for $Cr(CO)_4(tBu\text{-}dab)$.[38]

The high-energy absorption of $Cr(CO)_4(bpy)$ in the near-UV spectral region is only poorly resolved. In the C_2Cl_4/C_6H_6 (6/1, v/v) mixture, a broad band is apparent at 25 800 cm^{-1}, ϵ = 5734 M^{-1} cm^{-1}, while only a shoulder at 24 000−27 000 cm^{-1} occurs in C_6H_6 or toluene. Another maximum at 30 000 cm^{-1} (ϵ = 6650 M^{-1} cm^{-1}) superimposed on a strong broad absorption was observed[6] in C_6H_6. Both UV absorptions for the second unoccupied π^*_{bpy,a_2} and for π^*_{CO} orbitals, as well as bpy-localized intraligand transitions, are expected in this spectral region.[6,37,38] On excitation at 25 000 cm^{-1}, $Cr(CO)_4(bpy)$ shows in benzene solution[6,41] two weak emission bands at 16 000 and 12 850 cm^{-1}, respectively. They were assigned to emissions from two different MLCT states which, presumably, are in thermal equilibrium. Excited state lifetimes have not been reported.

$CrCO)_4(bpy)$ Excited States. The total CASSCF and CASPT2 energies obtained for the a^1A electronic ground state and the lowest singlet and triplet excited states of $Cr(CO)_4(bpy)$ on the basis of the 10e11a CASSCF space are reported in Table 1. The quality of the CASSCF active space with respect to the subsequent CASPT2 perturbation treatment is warranted by the nearly constant weights ω ($0.709 < \omega < 0.715$) of the CASSCF reference wave function in the final first-order CASPT2 wave function. The lower limit of the CASPT2 contribution to the correlation energy is 1.816 E_h for the a^1A_1 electronic ground state, in agreement with a better description of the correlation effects in this state at the CASSCF level and a larger ω (0.715) at the CASPT2 level. In the excited states, the CASPT2 correlation energy ranges between 1.835 and 1.846 E_h. The lowest excited states of $Cr(CO)_4(bpy)$ are nearly pure with CASSCF coefficients on the principal configuration greater than 0.80. The other configurations present in the CI expansion of

(34) Andersson, K.; Blomberg, M. R. A.; Fülscher, M. P.; Kellö, V.; Lindh, R.; Malmqvist, P. A.; Noga, J.; Olsen, J.; Roos, B. O.; Sadlej, A.; Siegbahn, P. E. M.; Urban, M.; Widmark, P.-O. MOLCAS-3. University of Lund, Sweden, 1994.
(35) Pitzer, R. *J. Chem. Phys.* **1973**, *58*, 3111.
(36) Stiddard, M. B. H. *J. Chem. Soc.* **1962**, 4712.
(37) Saito, H.; Fujita, J.; Saito, K. *Bull. Chem. Soc. Jpn.* **1968**, *41*, 359.
(38) Saito, H.; Fujita, J.; Saito, K. *Bull. Chem. Soc. Jpn.* **1968**, *41*, 863.
(39) Grevels, F. W.; Snoeck, T. L.; Stufkens, D. J.; Vlček, A., Jr. To be published.
(40) Staal, L. H.; Stufkens, D. J.; Oskam, A. *Inorg. Chim. Acta* **1978**, *26*, 255.
(41) Manuta, D. M.; Lees, A. J. *Inorg. Chem.* **1983**, *22*, 572.
(42) Finger, K.; Daniel, C. *J. Am. Chem. Soc.* **1995**, *117*, 12322.
(43) Daul, C.; Baerends, E. J.; Vernooijs, P. *Inorg. Chem.* **1994**, *33*, 3538.

Table 2. Calculated CASSCF and CASPT2 Excitation Energies (in cm^{-1}) for the Lowest Excited States of $Cr(CO)_4(bpy)$

one-electron excitation in the principal configuration		CASSCF	CASPT2
$a^1A_1 \rightarrow a^3B_2$	$3d_{x^2-y^2} \rightarrow \pi^*_{bpy,b_2}$	19 200	12 560
$a^1A_1 \rightarrow a^1B_2$	$3d_{x^2-y^2} \rightarrow \pi^*_{bpy,b_2}$	19 000	12 630
$a^1A_1 \rightarrow a^3B_1$	$3d_{yz} \rightarrow \pi^*_{bpy,b_2}$	17 970	13 630
$a^1A_1 \rightarrow a^1B_1$	$3d_{yz} \rightarrow \pi^*_{bpy,b_2}$	18 190	14 450
$a^1A_1 \rightarrow a^3A_1$	$3d_{xz} \rightarrow \pi^*_{bpy,b_2}$	21 590	15 800
$a^1A_1 \rightarrow b^1A_1$	$3d_{xz} \rightarrow \pi^*_{bpy,b_2}$	22 580	17 580
$a^1A_1 \rightarrow b^3B_1$	$3d_{x^2-y^2} \rightarrow 3d_{xy}$	28 400	24 080
$a^1A_1 \rightarrow b^3A_1$	$3d_{yz} \rightarrow \pi^*_{bpy,a_2}$	27 390	24 630
$a^1A_1 \rightarrow c^1A_1$	$3d_{yz} \rightarrow \pi^*_{bpy,a_2}$	28 720	25 370
$a^1A_1 \rightarrow c^3B_1$	$3d_{xz} \rightarrow \pi^*_{bpy,a_2}$	28 640	25 750
$a^1A_1 \rightarrow b^1B_1$	$3d_{xz} \rightarrow \pi^*_{bpy,a_2}$	29 140	26 200
$a^1A_1 \rightarrow b^3B_2$	$3d_{yz} \rightarrow 3d_{xy}$	32 460	28 230
$a^1A_1 \rightarrow c^1B_1$	$3d_{x^2-y^2} \rightarrow 3d_{xy}$	34 190	29 650
$a^1A_1 \rightarrow c^3A_1$	$3d_{x^2-y^2} \rightarrow 3d_{z^2}$	35 250	30 860
$a^1A_1 \rightarrow c^3B_2$	$3d_{xz} \rightarrow 3d_{z^2}$	36 790	31 530
$a^1A_1 \rightarrow b^1B_2$	$3d_{yz} \rightarrow 3d_{xy}$	38 540	32 230
$a^1A_1 \rightarrow c^1B_2$	$3d_{xz} \rightarrow 3d_{z^2}$	42 930	36 320
$a^1A_1 \rightarrow d^1A_1$	$3d_{x^2-y^2} \rightarrow 3d_{z^2}$	42 830	37 360

Table 3. Calculated Dipole Transition Moments (in au) Corresponding to the Ground State to Lowest Singlet State Electronic Transitions in $Cr(CO)_4(bpy)$

	transition	μ
MLCT(b_2)	$a^1A_1 \rightarrow a^1B_2$	0.02
	$a^1A_1 \rightarrow a^1B_1$	0.59
	$a^1A_1 \rightarrow b^1A_1$	2.39
MLCT(a_2)	$a^1A_1 \rightarrow c^1A_1$	−1.2
	$a^1A_1 \rightarrow b^1B_1$	−1.49
dd	$a^1A_1 \rightarrow c^1B_1$	0.33
	$a^1A_1 \rightarrow b^1B_2$	0.37
	$a^1A_1 \rightarrow c^1B_2$	−0.01
	$a^1A_1 \rightarrow d^1A_1$	0.15

the CASSCF solution correspond to double excitations in the d space of the metal and represent correlation effects. For the c^3B_2 and d^1A_1 excited states, the low coefficients of 0.67 and 0.69, respectively, express a mixing (or delocalization) of molecular orbitals which does not correspond to a mixing of states. On the contrary, the b^1B_2 and c^1B_2 states are characterized by a large state mixing. Indeed, the CI expansion of the CASSCF solution of the b^1B_2 state contains more than 20% of the c^1B_2 component and the expansion of the c^1B_2 state contains nearly 30% of the b^1B_2 component.

The CASSCF and CASPT2 calculated energies for excitation to the lowest excited states are reported in Table 2. At the CASSCF level, the excitation energies are overestimated by around 5000 cm^{-1} because of the neglect of the correlation dynamic effects. The lowest singlet MLCT states range between 12 630 and 17 580 cm^{-1} above the ground state, the corresponding triplets, nearly degenerate, lying between 12 560 and 15 800 cm^{-1}. They originate in the excitation of chromium d electrons to the lowest π^*_{bpy} orbital of b_2 local symmetry. Hereinafter, they will be denoted MLCT(b_2). Dipole transition moments calculated for individual MLCT excitations, reported in Table 3, show that the only transition expected to contribute importantly to the intense absorption band in the visible spectral region is the $a^1A_1 \rightarrow b^1A_1$ transition calculated at 17 580 cm^{-1}. This result agrees very well with experimental spectra, especially those measured in weakly solvating C_2Cl_4; vide supra. The MLCT transitions to the a^1B_1 and a^1B_2 excited states occur with dipole transition moments 4 and 120 times smaller, respectively. At most, they might contribute to the asymmetry of the absorption band and/or to the low-energy tail (between 12 820 and 14 710 cm^{-1}) observed in the solid state spectrum.

The calculated energy difference between b^1A_1 and b^3A_1, 1780 cm^{-1}, is smaller than the energy difference between the maxima of the absorption band and of the high-energy emission, 2900 cm^{-1}. This suggests that this emission occurs from the lower, presumably a^3B_1, state. The low-energy emission could then originate in the a^3B_2 state. Calculated energies of these states are 13 630 and 12 560 cm^{-1}, respectively. Their comparison with the experimental emission energies, 16 000 and 12 850 cm^{-1}, has to be only qualitative because of the solvent effect on the emission energies[6,40] and because of geometry relaxation effects which are not taken into account in the present calculations. However, a recent study, based on Gradient-CASSCF geometry optimization, of the relaxation effects in the lowest ^{3}MLCT of the model system $HMn(CO)_3(dab)$[44] seems to indicate a small deviation on going from the electronic ground state to the lowest ^{3}MLCT excited state. Such a heavy calculation cannot be performed on the large title complex.

The next excited states reported in Table 2 are of MLCT(a_2) type, corresponding to $3d \rightarrow \pi^*_{bpy,a_2}$ excitations and range between 25 370 and 26 200 cm^{-1} for the singlets and between 24 630 and 25 750 cm^{-1} for the triplets. The corresponding dipole transition moments associated with the singlets are reported in Table 3 and are around 2 times smaller than the dipole transition moment associated with the low-lying b^1A_1 MLCT state. The singlet excited states corresponding to $d \rightarrow d$ excitations are calculated between 29 650 and 37 360 cm^{-1}, in agreement with the experimental absorption spectra reported above. The associated dipole transition moments (Table 3) are 7−24 times smaller than the one calculated for the low-lying b^1A_1 MLCT state. The calculated energy (29 650 cm^{-1}) of the lower one of the two intense dd transitions, namely $a^1A_1 \rightarrow c^1B_1$, coincides with the absorption band at 30 000 cm^{-1} observed in benzene. These results show, however, that the intense absorption in the near-UV spectral region originates in strongly overlapping absorption bands due to closely spaced transitions into MLCT(a_2) and dd excited states, respectively. Both the energetic (Table 2) and intensity (Table 3) considerations indicate that the near-UV irradiation in the 355−400 nm range (28 169−25 000 cm^{-1}) used in previous photochemical and spectroscopic experiments[5,6,12−15] initially populated dominantly the MLCT(a_2) excited state(s), instead of the dd ones. The c^1B_2 excited state corresponding to the $3d_{xz} \rightarrow 3d_{z^2}$ excitation has been proposed as photoactive in the mechanism of the efficient CO loss under UV irradiation.[13] However, its energy, calculated at 36 320 cm^{-1}, is far too high compared with the maximum excitation energy used in photochemical studies, 27 630 cm^{-1}. Although the c^1B_2 state obviously was not populated by the optical excitation, its mixing with one or several low-lying (singlet) MLCT states at the early stage of the reaction path corresponding to the CO loss could be responsible for the observed primary reaction.[13] Such a mixing between dissociative and quasi-bound excited states has been shown to lead to the M−H homolysis in $HM(CO)_3$(α-diimine) complexes.[42]

The calculated singlet−triplet (S−T) energy splitting is rather small for MLCT states, 1780 cm^{-1} for b^1A_1, while much smaller values, 820 and 70 cm^{-1}, were obtained for the aB_1 and aB_2 states, respectively. Also the MLCT(a_2) states show small values of S−T splittings, 740 and 450 cm^{-1}. On the contrary, the S−T splitting is much larger for the dd excited states, ranging from 4000 cm^{-1} for bB_2 to 6500 cm^{-1} for $d^1A_1-c^3A_1$ states. Despite the differences in the S−T splittings, the lowest triplet dd state, b^3B_1, is 6500 and 8280 cm^{-1} above the highest singlet and triplet MLCT(b_2) states, respectively, and even much more above some of the excitation energies used in the photochemical experiments.[12] The energy differences between dd and MLCT(b_2) states are also much higher than the activation energies, 1349−1426 cm^{-1} measured[12] for the photodissociation

(44) Guillaumont, D.; Daniel, C. *Chem. Phys. Lett.* **1996**, *257*, 1.

Table 4. Comparison between the CASPT2 Energies of Excitation to the Lowest Singlet States of $Cr(CO)_4(L)$ (L = dab, bpy) Using Various Computational Strategies

one-electron excitation in the principal configuration		L			
		bpy (CASPT2)	dab (CASPT2)	dab(CASSCF/CCI)	with Davidson correction
$a^1A_1 \rightarrow a^1B_2$	$3d_{x^2-y^2} \rightarrow \pi^*_{dab}$	12 630	6 900	7 630	7 180
$a^1A_1 \rightarrow a^1B_1$	$3d_{yz} \rightarrow \pi^*_{dab}$	14 450	9 500	9 580	9 845
$a^1A_1 \rightarrow b^1A_1$	$3d_{xz} \rightarrow \pi^*_{dab}$	17 580	15 920	17 450	16 720
$a^1A_1 \rightarrow b^1B_1$	$3d_{x^2-y^2} \rightarrow 3d_{xy}$	29 650	27 415	27 980	27 140
$a^1A_1 \rightarrow b^1B_2$	$3d_{yz} \rightarrow 3d_{xy}$	32 230	30 895	32 850	30 180

(1) induced by MLCT excitation. The results of the present calculations support the earlier conclusions[12,13] that the CO dissociation induced by irradiation into the MLCT absorption band cannot be explained by a back-population of a dissociative dd state from a ^{3}MLCT(b_2), or even a ^{1}MLCT(b_2), state.

$Cr(CO)_4L$ (L = dab) Excited States. Comparison between the CASPT2 excitation energies of the lowest singlet states of $Cr(CO)_4$(bpy) and the excitation energies of the corresponding states of the model system $Cr(CO)_4$(dab) are reported in Table 4. The most significant feature is the lowering of the MLCT excited states on going from the bpy containing molecule to its dab analog. Indeed, the energies for excitation to the lowest MLCT states follow the degree of conjugation within the π acceptor ligand. A low degree of conjugation will lower the MLCT excited states by more than $^1/_2$ eV, while, obviously, the metal-centered excited states will be less affected by this π-acceptor effect. An illustration is given by the calculated low-energy shift (1660 cm^{-1}) for the $a^1A_1 \rightarrow b^1A_1$ transition, which agrees rather well with the observed red shift of 1200 cm^{-1} on going from $Cr(CO)_4$(bpy) to $Cr(CO)_4$(tBu-dab) in a benzene solution. According to the results reported in Table 4, the less crowded $Cr(CO)_4$(dab) molecule could be used as a model system for the study of metal-centered (dd) excited state photoactivity, but under no circumstances could it model the photodissociation of the bpy complex through MLCT activation.

Conclusion

This work represents the first quantitative study based on ab initio calculations of the electronic structure of the lowest excited states of a transition metal complex with a large π-acceptor ligand used in photochemical experiments. The intense solvatochromic absorption band observed in the visible region (between 17 700 and 19 750 cm^{-1}) is attributed to the $a^1A_1 \rightarrow b^1A_1$ ^{1}MLCT transition calculated at 17 580 cm^{-1} with a dipole transition moment 4−120 times larger than for the other MLCT states found in the same energy domain. The high-energy absorption feature in the near-UV spectral region between 24 000 and 27 000 cm^{-1} is assigned to the second series of ^{1}MLCT states corresponding to excitations of chromium d electrons to the π^*_{bpy} orbital of a_2 local symmetry. The metal-centered spin-singlet excited states corresponding to dd excitations occur between 29 650 and 37 360 cm^{-1} and may contribute indirectly to the efficient CO loss through their mixing with the low-lying MLCT states at the early stage of the dissociation. The singlet and triplet components of the MLCT states are nearly degenerate ($\Delta S-T \leq 1000$ cm^{-1}) except for the $a^3A_1-b^1A_1$ states, for which the singlet−triplet energy gap is rather large (2000 cm^{-1}) due to a strong destabilizing interaction between the a^1A_1 electronic ground state and the b^1A_1 component. The same trends have been obtained in a recent density functional study of the MLCT states of the $[Ru(bpy)_3]^{2+}$ ion.[43] The lowest ^{3}MLCT states calculated at 12 560 and 13 630 cm^{-1} are probably responsible for the emission observed in this energy range.

The photoreactivity of $Cr(CO)_4$(bpy) under different conditions of irradiation may be analyzed through the main features of the theoretical spectrum, which is characterized by three well-separated and well-defined spectral regions: (i) a first series of MLCT states between 12 560 and 17 580 cm^{-1} corresponding to $3d \rightarrow \pi^*_{bpy,b_2}$ excitations; (ii) a second series of MLCT states between 24 630 and 26 200 cm^{-1} corresponding to $3d \rightarrow \pi^*_{bpy,a_2}$ excitations; (iii) an upper domain of the spectrum between 28 230 and 37 360 cm^{-1} assigned to metal-centered transitions corresponding to $d \rightarrow d$ excitations. Irradiation under visible light will bring the system into the low-lying MLCT states presumably quasi-bound with respect to the CO loss. The presence of late energy barriers along the reaction path, due to avoided crossings between these low-lying MLCT states and upper dissociative states,[13] will govern the low-energy reactivity. The efficiency of reaction 1 will depend on the facility for the system to overcome these barriers either in a direct fashion, or through tunneling. These processes will compete with the deactivation through intersystem crossing to the low-lying ^{3}MLCT states followed by nonradiative and inefficient radiative deactivation to the ground state. Irradiation under 355 nm (28 170 cm^{-1}) in the near-UV region will populate the second series of MLCT(a_2) states near the higher dissociative metal-centered excited states. The interaction between the dissociative states and these MLCT(a_2) states may generate energy barriers at the early stage of the reaction pathway corresponding to the CO loss. The system will have sufficient vibrational energy to overcome these energy barriers and reach the dissociative part of the corresponding potentials in order to dissociate efficiently on a very short time scale (a few hundred of femtoseconds). Such a mechanism, based on a simulation of the photodissociation dynamics through wavepacket propagation,[45] has been proposed for an efficient M−R homolysis in the model system $HMn(CO)_3$(dab) under irradiation in the near-UV energy domain. A detailed knowledge of the potential energy curves calculated for the CO loss in $Cr(CO)_4$(bpy) is necessary confirm this mechanism.

Acknowledgment. The authors are grateful to Dr. M. Fülscher and Dr. K. Pierloot for helpful discussions and for providing a level shift corrected version of the CASPT2 program. This work was supported by European Concerted Action COST D4 on "Design and preparation of new molecular systems with unconventional electrical, optical and magnetic properties". The calculations were carried out on the C98 computer and on the IBM/RS 6000 workstations of the IDRIS (Orsay, France) through a grant of computer time for the Conseil Scientifique de l'Institut du Développement et des Ressources en Informatique Scientifique.

IC960872V

(45) Finger, K.; Daniel, C.; Saalfranck, P.; Schmidt, B. *J. Phys. Chem.* **1996**, *100*, 3368.